

Iron-based superconductors: Magnetism, superconductivity, and electronic structure (Review Article)

A. A. Kordyuk^{a)}

Institute of Metal Physics, National Academy of Sciences of Ukraine, 36 Vernadsky Str., Kiev 03142, Ukraine
(Submitted May 18, 2012)

Fiz. Nizk. Temp. **38**, 1119–1134 (September 2012)

Angle resolved photoemission spectroscopy (ARPES) reveals the features of the electronic structure of quasi-two-dimensional crystals which are crucial for spin and charge ordering and determine the mechanisms of electron–electron interactions, including superconducting pairing. The newly discovered iron-based superconductors (FeSC) promise interesting physics stemming, on one hand, from a coexistence of superconductivity and magnetism and, on the other, from a complex multi-band electronic structure. In this review I want to offer a simple introduction to the physics of FeSC, and to argue that all the complexity of FeSC properties is encapsulated in their electronic structure. For many compounds, this structure has been determined on the basis of numerous ARPES experiments and agrees reasonably well with the results of band structure calculations. Nevertheless, the existing small differences may help to understand the mechanisms of magnetic ordering and superconducting pairing in FeSC. © 2012 American Institute of Physics. [<http://dx.doi.org/10.1063/1.4752092>]

1. Introduction

The discovery four years ago of $\text{LaO}_{1-x}\text{F}_x\text{FeAs}$,¹ a new superconductor with a transition temperature of 26 K, marked the beginning of a new era in research on superconductivity. The Copper Age has been replaced by the Iron Age, i.e., all the researchers and funding have switched from the high- T_c cuprates (HTSC or CuSC) to the iron-based superconductors (FeSC), as is clear from a number of early reviews.^{2–8} Today, after four years of active research, Ref. 1 has been cited more than 3000 times and research on FeSC is in the mainstream of condensed matter physics.^{9–12}

There are several good reasons why FeSC are so interesting. First, they promise interesting physics that stems from the coexistence of superconductivity and magnetism. Second, they provide a much wider variety of compounds for research and, with their multi-band electronic structure, they offer the hope of finally discovering the mechanism of high-temperature superconductivity and finding the way to increase T_c . Lastly, the FeSC are quite promising for applications. Having much higher H_c than cuprates and high isotropic critical currents,^{13–15} they are attractive for electrical power and magnetic applications, while the coexistence of magnetism and superconductivity makes them interesting for spintronics.¹⁶

To date, there are a number of useful and comprehensive reviews of the diverse properties of FeSC (Refs. 2–5 and 7–9) and on pairing models.^{9,11,12} The scope of this review is smaller but twofold. On one hand, I want to give a simple, even oversimplified introduction to FeSC physics. On the other hand, I want to argue that all the complexity of the FeSC properties is encapsulated in their intricate but well defined and rather common multi-band electronic structure. This structure has been found for many compounds by means of angle resolved photoemission experiments (ARPES), and one of the purposes of this review is to show that, while the overall agreement between the measured and calculated band structures is very good, it is the observed small differences¹⁷ that may help to understand the mecha-

nisms of the magnetic ordering and superconducting pairing in FeSC.

2. Iron-based superconductors

Many families of FeSC with different structures and compositions are already known,^{2–5,7–9} but all share a common iron-pnictogen (P, As) or iron-chalcogen plane (Se, Te), as shown in Fig. 1.⁸ All these compounds have a similar electronic band structure in which the electronic states at the Fermi level are occupied predominantly by Fe 3d electrons. The structure itself is quite complex and, in most cases, consists of five conduction bands that result in rather complex fermiology that changes rapidly with doping and, consequently, leads to many unusual superconducting and normal state properties. Figure 2 shows the square FeAs lattice and the corresponding Fermi surface for a stoichiometric parent compound. Figure 3 provides examples of the FeSC phase diagrams with distinct areas of the antiferromagnetically

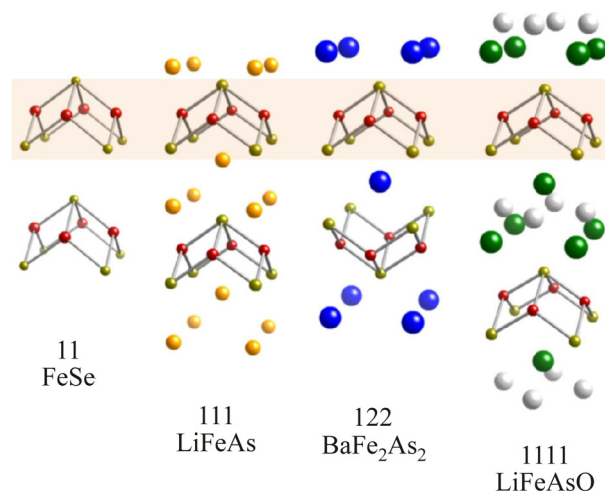


FIG. 1. Crystal structures of some of iron-based superconductors, after Ref. 8.

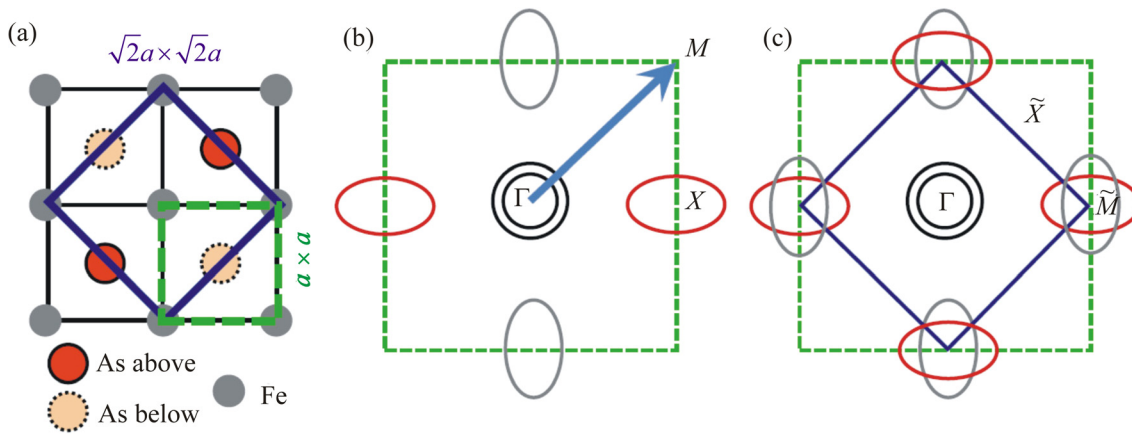


FIG. 2. (a) FeAs lattice indicating As above and below the Fe plane. Dashed green and solid blue squares indicate 1- and 2-Fe unit cells, respectively. (b) Schematic 2D Fermi surface in the 1-Fe BZ whose boundaries are indicated by a green dashed square. (c) Fermi sheets in the folded BZ whose boundaries are now shown by a solid blue square. After Ref. 11.

ordered spin density wave (marked as AFM or SDW and bordered by the Néel temperature T_N) and superconducting (SC, T_c) phases, which resembles the extensively discussed phase diagram of CuSC.¹⁸ Here I briefly review some of the most interesting and most studied FeSC materials with references to their properties and experimental (ARPES) studies of their electronic structure, which will be important for the following discussion.

1111. Starting with $\text{LaO}_{1-x}\text{F}_x\text{FeAs}$,¹ the 1111 family holds the record for T_c : NdFeAsO_{1-y} (54 K), $\text{SmFeAsO}_{1-x}\text{F}_x$ (55 K), $\text{Gd}_{0.8}\text{Th}_{0.2}\text{FeAsO}$ (56.3 K), but the material is hard to study. First, the available single crystals are too small—for all members of the family they only grow as thin wafers up to $200 \times 200 \times 10 \mu\text{m}$.¹⁴ Second, the end of the crystal reveals a polar surface with distinct surface states that are markedly different from the bulk electronic structure²³ and greatly complicate the use of any surface sensitive experimental probe such as ARPES.²⁴

122. The 122 family consists of a variety of different compounds with wide ranges of doping in both hole and elec-

tron sides⁹ that form a rich phase diagram (see Fig. 3) where the superconductivity and magnetism compete or coexist. The most studied compounds are the hole doped $\text{Ba}_{1-x}\text{K}_x\text{Fe}_2\text{As}_2$ (BKFA) with $T_c^{\text{max}} = 38 \text{ K}$ ²⁵ and the electron doped $\text{Ba}(\text{Fe}_{1-x}\text{Co}_x)_2\text{As}_2$ (BFCA), 22 K.^{26,27} Both share the same parent compound, BaFe_2As_2 (BFA), which is a compensated metal, i.e., the total volume of its three hole Fermi surfaces (FS's) is equal to the total volume of two electron FS's.^{28,29} BFA goes into a magnetically ordered phase below 140 K (Ref. 30) and never superconducts. An extremely overdoped BKFA is a stoichiometric KFe_2As_2 (KFA),³¹ which is non-magnetic, with $T_c = 3 \text{ K}$. There is also an interesting case of isovalent doping, $\text{BaFe}_2(\text{As}_{1-x}\text{P}_x)_2$ (BFAP) ($T_c = 30 \text{ K}$)²² with a similar phase diagram (see Fig. 3).

To this, one can add a number of similar compounds: $\text{Ba}_{1-x}\text{Na}_x\text{Fe}_2\text{As}_2$ (BNFA) ($T_c^{\text{max}} = 34 \text{ K}$),^{32,33} $\text{Ca}_{1-x}\text{Na}_x\text{Fe}_2\text{As}_2$ ($\sim 20 \text{ K}$),³⁴ CaFe_2As_2 ($T_N = 170 \text{ K}$, $T_c > 10 \text{ K}$ under pressure),³⁵ $\text{EuFe}_2(\text{As}_{1-x}\text{P}_x)_2$ ($T_c = 26 \text{ K}$),³⁶ etc.⁷

As a consequence of good crystal quality and the variety of its compounds, the 122 family is the most studied by ARPES³⁷

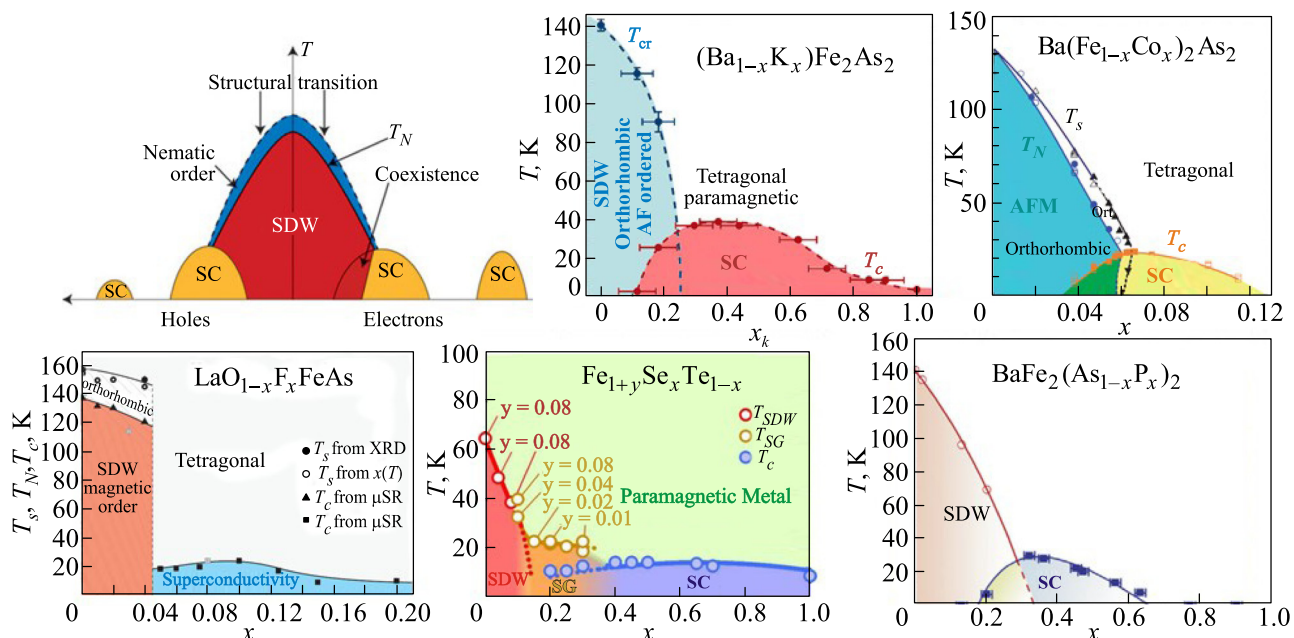


FIG. 3. Examples of the FeSC phase diagrams: a schematic one,¹² and the diagrams measured for $(\text{Ba}_{1-x}\text{K}_x)\text{Fe}_2\text{As}_2$,⁹ $\text{Ba}(\text{Fe}_{1-x}\text{Co}_x)_2\text{As}_2$,¹⁹ $\text{La}(\text{O}_{1-x}\text{F}_x)\text{FeAs}$,²⁰ $\text{Fe}_{1+y}\text{Se}_x\text{Te}_{1-x}$,²¹ $\text{BaFe}_2(\text{As}_{1-x}\text{P}_x)_2$.²²

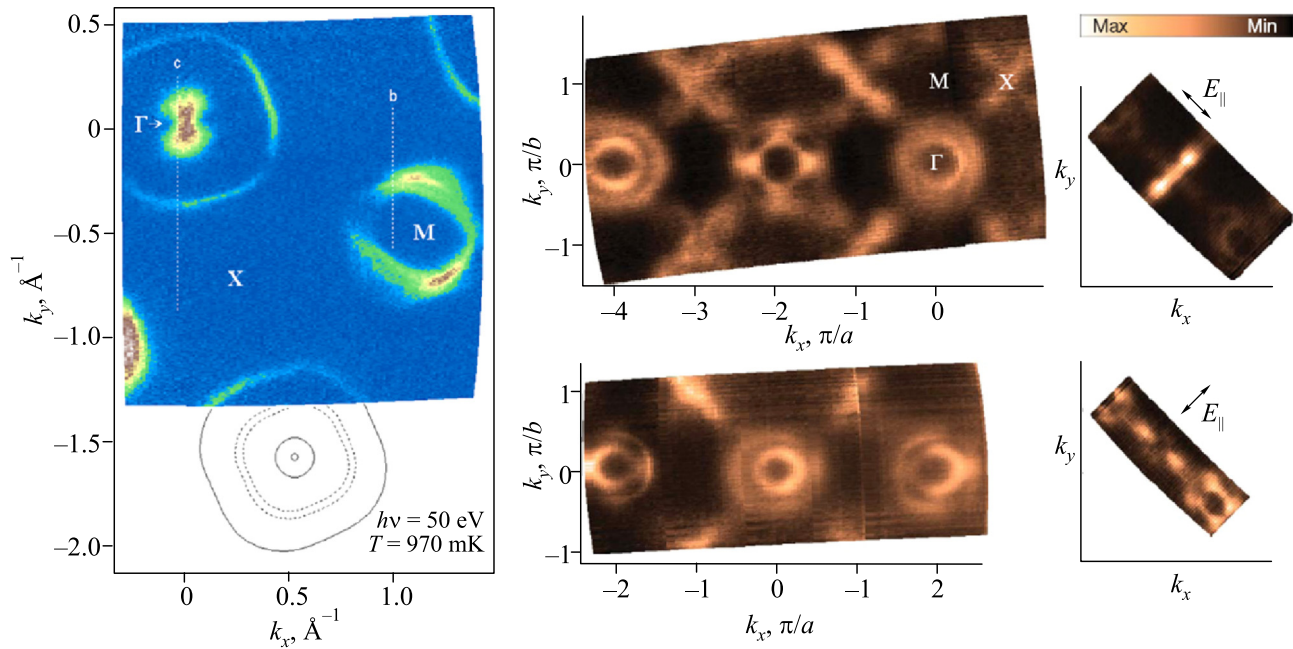


FIG. 4. Fermi surface (FS) maps measured by ARPES for LiFeAs (Ref. 62) (left) and optimally doped $\text{Ba}_{1-x}\text{K}_x\text{Fe}_2\text{As}_2$ (BKFA).⁴⁰

(see Refs. 38–44 for BKFA, Refs. 28, 45–49 for BFA, Refs. 29, 50–53 for BFA, Refs. 31 and 54 for KFA, Refs. 29 and 55 for CaFe_2As_2 , Refs. 56 and 57 for BFAP, and Ref. 58 for $\text{EuFe}_2(\text{As}_{1-x}\text{P}_x)_2$). The ARPES spectra represent the bulk electronic structure of this family well, at least for the hole doped BKFA, BNFA, and BFAP, where the superconducting gap is routinely observed^{39,41,59} and is in a good agreement with bulk probes.^{43,44} This makes the 122 family a favorite for study of the rich physics of the iron-based superconductors.

111. As it is highly reactive with air and, consequently, more challenging to study, the 111 family yields many interesting results. The main representative of the family, LiFeAs,^{60,61} is the most “arpesable” compound.^{62–64} It grows in good quality single crystals⁶⁵ that cleave between the two Li layers, thus revealing a non-polar surface with protected topmost FeAs layer; it is stoichiometric, i.e. impurity clean; it has a transition temperature of about 18 K and one can measure the superconducting gap by ARPES and compare the result with that derived from bulk techniques. It is non-magnetic so that the observed band structure is free of SDW replicas and, finally, its electronic bands are the most widely separated from each other so they can easily be disentangled in order to analyze their fine structure.⁶³ Figure 4 shows the FS maps measured by ARPES for LiFeAs (left) and an optimally doped BKFA (right).

NaFeAs is another member of the 111 family. It shows three successive phase transitions at around 52, 41, and 23 K, which correspond to structural, magnetic, and superconducting transitions, respectively.^{66,67} The compound is less reactive with the environment than LiFeAs but exposure to air strongly affects T_c .⁶⁸ Replacing Fe by either Co or Ni suppresses the magnetism and enhances superconductivity.⁶⁹ For ARPES on NaFeAs, see Refs. 70 and 71.

11. The binary FeAs does not crystallize into an FeAs layered structure (it adopts an orthorhombic structure consisting of distorted FeAs_6 octahedra, unlike the superconducting ferro-pnictides in which FeAs_4 tetrahedra form

square lattices of iron atoms⁷²), but FeSe does. So, the 11 family is presented by simplest ferro-chalcogenides FeSe and FeTe, and their ternary combinations $\text{FeSe}_x\text{Te}_{1-x}$.⁷³ FeSe becomes superconducting at approximately 8 K,⁷⁴ and up to 37 K under pressure.⁷⁵ $\text{Fe}_{1+y}\text{Se}_x\text{Te}_{1-x}$ has a maximum T_c of about 14 K for $x=0.5$.^{21,73,76} In crystals grown with excess (y) Fe atoms in amounts beyond those needed to fill the Fe square lattice layers they go into interstitial positions within the Te layers.⁷ For ARPES data on the 11 family, see Refs. 77–80.

245 or x22. Attempts to intercalate FeSe, the simplest FeSC, resulted in discovery of a new family $\text{A}_x\text{Fe}_{2-y}\text{Se}_2$ (A stands for an alkali metal: K, Rb, Cs, Tl) with T_c up to 30 K and with exceptionally high Néel temperature (>500 K) and magnetic moment ($>3\mu_B$).^{81–83} This family is most often called “245” because of its parent compound $\text{A}_{0.8}\text{Fe}_{1.6}\text{Se}_2 \equiv \text{A}_2\text{Fe}_4\text{Se}_5$. It is interesting that the resistivity shows insulating behavior down to 100 K and superconductivity seems to develop from an antiferromagnetic semiconductor.⁸⁴ This, however, is not consistent with ARPES data which indicate the presence of a Fermi surface.^{85–88} It is even more interesting that the observed FS is completely electron-like, which seems to contradict the most popular $s\pm$ scenario for superconducting pairing.^{9,11,12} Recently, it has been shown,⁸⁹ that the puzzling behavior of these materials is the result of separation into metallic and antiferromagnetic insulating phases, of which only the former becomes superconducting, while the latter has hardly any relation to superconductivity. The superconducting phase has an electron doped composition $\text{A}_x\text{Fe}_2\text{Se}_2$ (so, the family can be called “x22”). A similar conclusion follows from neutron scattering experiments.⁹⁰

3. Magnetism

The magnetic properties of the FeSC are, of course, very rich and far from completely understood,⁹¹ but since the

focus of this review is on superconductivity, I shall discuss only two issues: the coexistence of static magnetism and superconductivity and the role of spin fluctuations.

3.1. Magnetic ordering

The nearly perfect FS nesting in many parent compounds (which are compensated metals) suggests a static density wave with the nesting vector (π, π) as a way to lower the kinetic energy of the electrons (Peierls transition).⁹² Therefore, an antiferromagnetic spin density wave in those compounds is quite natural—the easiest ordering for an Fe lattice is the spin ordering.⁹³ Indeed, almost all the parent compounds have an antiferromagnetic SDW below the Néel temperature with exactly the same wave vector. This most common spin configuration of the Fe atoms is shown in Fig. 5 (left).⁹⁴ This said, there is some controversy regarding the importance of the interactions of the localized spins.^{6,91,95,96} From experiment, there are both pro and con arguments on this problem. Pro: when the FS nesting is good (BFA^{29,50,52} and other parent compounds of 122 family,^{56–58} NaFeAs^{70,71}), an SDW is present, and when nesting is poor or absent (superconducting BKFA,^{38,39} BFCA,^{28,45} BFAP,⁵⁶ and stoichiometric LiFeAs⁶²), there is no magnetic ordering. Con: Fe_{1+y}Te shows different spin order, see Fig. 5 (right),⁹⁴ despite having very similar FS topology (as implied by calculations⁹⁷ and ARPES studies⁷⁷). So, one may conclude that the mechanism for the magnetic ordering in FeAS is not yet clear, but for the scope of this review it is important to know that this ordering is routinely observed in many compounds, always adjacent to a superconducting phase and often coexisting with it.

Since static magnetism and superconductivity coexist on the phase diagrams for a number of FeSC,¹⁰ it is important to answer the following questions: (1) do they coexist microscopically and (2) do magnetism and superconductivity evolve from the same conduction electrons? The latter is related to the “itinerant vs. localized” problem and was briefly discussed above. The problem of coexistence on the microscopic scale is related to sample homogeneity and has been addressed in a number of publications.¹⁰ In particular, for BFCA crystals, the homogeneity of superconducting state was demonstrated by magneto-optic imaging⁹⁸ down to 2 μm and by NMR⁹⁹ down to the sub-nanometer scale. Another 122 compound, BKFA, is known to be inhomogene-

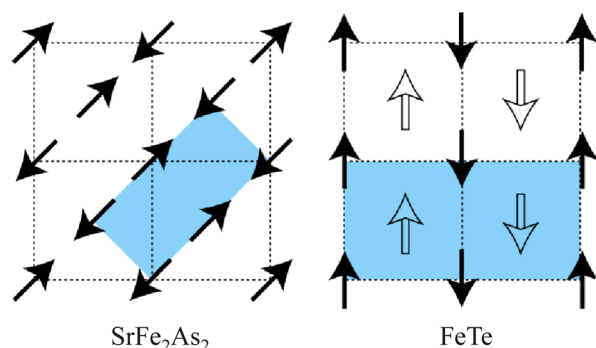


FIG. 5. In-plane magnetic structure common for the 1111 and 122 parent compounds (left) and for parent 11 compound (FeTe, right). The shaded areas indicate the magnetic unit cells. After Ref. ⁹⁴.

ous,⁴¹ and some separation of the magnetic and superconducting regions has been found on a nanometer scale.¹⁰⁰ Evidence of homogeneity has been reported for one of the 245 family, $\text{K}_{0.8}\text{Fe}_{1.6}\text{Se}_2$,¹⁰¹ but not confirmed by magnetic measurements on similar samples.¹⁰² Clear phase separation in other, Rb based 245 compounds, has recently been revealed by ARPES⁸⁹ and by inelastic neutron scattering (INS).⁹⁰ It has been shown, that, as in the quaternary borocarbides,¹⁰⁴ in EuFe_2As_2 under pressure¹⁰³ antiferromagnetism is realized on the Eu sublattice and affects the superconductivity on the Fe sublattice. So, one may conclude that while on some systems like 245 the magnetic and superconducting phases are spatially separated, the question of coexistence in other FeSC systems requires more careful study.

There is another closely related and interesting issue. FeSC are perfect systems for realization of the CDW (or SDW) induced superconductivity, as was suggested long ago^{105–107} and widely discussed.^{108–111} For a slightly non-stoichiometric system, the band gap cannot kill the FS completely since some extra carriers should form small FS pockets and place the van Hove singularity (vHs) close to the Fermi level. This mechanism is supported empirically since there are many known systems where superconductivity occurs at the edge of CDW or SDW phase.^{112–114} On the other hand, the related increase of the density of states seems to be too small to explain the observed T_c with the standard BCS model. In this sense, the argument regarding importance of the proximity of FS to Lifshitz transition for superconductivity can help to understand density wave induced superconductivity, in general.

3.2. Spin-fluctuations

If a magnetically mediated pairing mechanism takes place in FeSC, the spin-fluctuation spectrum must contain the necessary spectral weight to facilitate pairing.⁹¹ It is also expected that fingerprints of its structure will be recognizable in the one-particle spectral function, as in case of cuprates.^{115,116}

The spin dynamics in the FeSC is revealed primarily by INS, supplemented in some cases by NMR measurements.⁹¹

First, a correlation between the spectral weight of the spin-fluctuations and superconductivity is observed. In at least two cases (BFCA^{117,118} and $\text{LaFeAsO}_{1-x}\text{F}_x$ (Ref. ¹¹⁹)), when antiferromagnetically ordered parent compounds are overdoped by electron doping, the spin fluctuations vanish together with the FS hole pocket²⁸ and superconductivity. This is compatible with the idea that the spin fluctuations are completely defined by the electronic band structure and play an important role in superconductivity.

Second, the correlation between the normal state spin excitations and electronic structure is found to be common for all FeSC.⁹¹ In particular, even in $\text{Fe}_{1+y}\text{Se}_x\text{Te}_{1-x}$,¹²⁰ an interesting early development in the study of the spin excitations was that, in contrast to the parent FeTe, the spin fluctuations in superconducting samples were found at a wave vector similar to that found in other Fe-based materials. Also, there is another common feature, a quartet of low-energy incommensurate inelastic peaks characterized by the square lattice wave

vectors ($\pi \pm \xi$, π) and (π , $\pi \pm \xi$), observed for BFCA,^{121,122} $\text{Fe}_{1+y}\text{Se}_x\text{Te}_{1-x}$,¹²³ and CaFe_2As_2 ,¹²⁴ analogously to CuSC.¹²⁵

Third, a “resonance peak” in the spin-fluctuation spectrum has been observed in many FeSC compounds in superconducting state, and is regarded by many authors as evidence of a sign change of the superconducting order parameter.^{10,91}

The spin resonance, a resonance in the dynamic spin susceptibility, occurs indeed because of its divergence through a sign change of the superconducting order parameter on different parts of the Fermi surface.¹²⁶ In cuprates, it has been associated with the “resonance peak,” observed in INS experiments, and considered as one of the arguments for *d*-wave symmetry of the superconducting gap. In FeSC, the resonance peak was predicted to be the most pronounced for the $s\pm$ gap^{127,128} and, indeed, peaks in INS spectra have been observed for a number of compounds: BKFA,¹²⁹ BFCA,^{130,131} $\text{Fe}_{1+y}\text{Se}_x\text{Te}_{1-x}$,^{123,132} $\text{Rb}_2\text{Fe}_4\text{Se}_5$,^{90,133} etc.⁹¹ However, one should realize that the peak in the dynamic susceptibility is not necessarily caused by the spin resonance but can be related to a peak in the bare susceptibility (Lindhard function), which, as a result of self-correlation of the electron Green function, is expected to be peaked in energy at about 2Δ and in momentum at the FS nesting vectors.¹³⁴ In Ref. 135, in contrast to,¹²⁸ it has been shown that a prominent hump structure appears just above the spectral gap by taking into account the quasiparticle damping in SC state. The resulting hump structure looks similar to the resonance peak in the $s\pm$ -wave state, although the height and weight of the peak in the latter state are much larger. This shows that in order to support the sign change scenario, not only the presence of the peak in INS spectra but also its spectral weight should be considered. The latter is not trivial task. In Ref. 131, for example, the INS measurements were calibrated in the absolute scale and the spectral weight of the resonance in BFCA has been found to be comparable to ones in cuprates.

In summary, the spin-fluctuation spectra in FeSC, look, at first glance, similar to the ones in CuSC in terms of appearance and correlation with electronic structure, but an accurate interpretation requires further effort. As the latest example of this, a combined analysis of neutron scattering and photoemission measurements on superconducting $\text{FeSe}_{0.5}\text{Te}_{0.5}$ (Ref. 132) has shown that, while the spin resonance occurs at an incommensurate wave vector compatible with nesting, neither spin-wave nor FS nesting models can describe the magnetic dispersion. The authors propose a coupling of spin and orbital correlations as key to explaining this behavior.

3.3. Pseudogap

Surprisingly, the pseudogap in FeSC is not as popular a topic as with the cuprates.¹³⁶ From a nearly perfect FS nesting one would expect a pseudogap owing to incommensurate ordering as in the transition metal dichalcogenides¹³⁷ and, maybe, in cuprates.¹³⁸ If the pseudogap in cuprates is caused by superconducting fluctuations,¹³⁹ then it would be also natural to expect this in FeSC.

In NMR data, the decrease in $1/T_1T$ in some of the 1111 compounds and BFCA⁵ has been associated with the pseudo-

gap. The interplane resistivity data for BFCA over a broad doping range also shows a clear correlation with the NMR Knight shift, ascribed to the formation of the pseudogap.¹⁴⁰ In SmFeAsO_{1-x} , the pseudogap has been determined from resistivity measurements.¹⁴¹ Evidence of superconducting pairs in the normal state (up to $T \approx 1.3T_c$) has been obtained using point-contact spectroscopy on BFCA film.

Evidence of a pseudogap has been reported on the basis of photoemission experiments on polycrystalline samples^{142,143} and some ARPES experiments on single crystals,¹⁴⁴ but many other ARPES studies^{41,42,57,59,64,145,146} and STM measurements^{147,148} do not support this. The absence of a pseudogap in the ARPES spectra may just be a consequence of low spectral weight modulation by the magnetic ordering which may reduce its importance for superconductivity, as discussed in Sec. 3.2.

4. Superconductivity

In 1111 and 122 systems, superconductivity arises with electron or hole doping, or can be induced by pressure¹⁴⁹ or by isovalent doping. In 111 systems, superconductivity already emerges at zero doping instead of magnetic order (in LiFeAs) or together with it (in NaFeAs). There are several important experimentally established tendencies, exhibited by many representatives of the iron-based family with highest values of T_c (Ref. 146): a large difference in the size of the superconducting gap on different FS pockets,^{39,43,150,151} values of Δ/T_c similar to the cuprates and much higher than expected from BCS,^{43,59,150} and correlation of T_c with anion height.¹⁵² The complexity of the electronic structure of FeSC was originally an obstacle on the way to its understanding,^{39,40} but on closer examination, this variety in the electronic states turned out to be extremely useful for uncovering the correlation between orbital character and pairing strength¹⁴⁶ and, more generally, between electronic structure and superconductivity.¹⁷ In this section I briefly discuss the existing pairing models, the experimental (mainly ARPES) data on the symmetry of the superconducting gap, and the observed general correlation of the electronic band structure with T_c .

4.1. Pairing models

Based on the similarity of the phase diagrams for FeSC and cuprates, it has been proposed that the pairing in FeSC is also mediated by spin-fluctuations with a sign change in the superconducting order parameter. Then, to acquire the FS geometry of the FeSC, the symmetry of the sign change should be different from *d*-wave symmetry of cuprates and can be satisfied by an extended *s*-wave pairing with a sign reversal of the order parameter between different Fermi surface pockets.¹⁵³ Today, most researchers believe that the gap has $s\pm$ symmetry, at least in lightly and optimally doped FeSCs.^{11,12}

This said, numerous studies of superconductivity in FeSCs demonstrate that the physics of the pairing could be more complicated than it originally thought because of the multiorbital/multiband nature of low-energy electronic excitations.¹² It turns out that both the symmetry and the structure of the pairing gap result from a rather nontrivial interplay between spin-fluctuation exchange, Coulomb

repulsion, and the momentum structure of the interactions. In particular, an $s\pm$ -wave gap can be with or without nodes, depending on the orbital content of low-energy excitations, and can even evolve into a d -wave gap with hole or electron overdoping. In addition to spin fluctuations, FeSCs also possess charge fluctuations that can be strongly enhanced^{96,154} owing to proximity to a transition into a state with orbital ordering. This interaction can give rise to a conventional s -wave pairing.

The experimental data on superconductivity show very rich behavior, superconducting gap structures appear to vary substantially from family to family, and even within families as a function of doping or pressure.¹¹ The variety of different pairing states raises the issue of whether the physics of FeSCs is model dependent or is universal, governed by a single underlying pairing mechanism.¹²

In favor of $s\pm$ symmetry, there are the natural expectation that spin-fluctuations mediate pairing in FeSC, the observation of spin resonances by INS, which implies a sign change of Δ as discussed above, and numerous experimental indications of a nodal gap^{57,155,156} (also see the references in Refs. 11 and 12). It has also been argued¹⁵⁷ that the very presence of a region of coexistence of SC and stripe magnetism in the FeSCs is a fingerprint of an $s\pm$ gap, because a first-order transition between a pure magnetic and a pure SC state is much more likely for an s^{++} gap.¹²

On the other hand, several contrary arguments come from ARPES. There is evidence of strong electron-phonon coupling in LiFeAs.^{63,64} The accurately measured gap anisotropy is difficult to reconcile with the existing $s\pm$ models but can be with s^{++} models based on orbital fluctuations assisted by phonons.^{154,158,159} The remnant superconductivity in KFe_2As_2 , and, actually, for all overdoped BKFA started from the optimally doped one,⁴⁰ should have different symmetry since only hole like FSs are present.¹⁷ The same is holds for $\text{A}_x\text{Fe}_{2-y}\text{Se}_2$ where only electron-like FSs are present.^{85–89}

It has been suggested¹² that in both $\text{A}_x\text{Fe}_{2-y}\text{Se}_2$ and KFe_2As_2 the gap symmetry may be d -wave, though with different nodes. In Ref. 160 it is argued that $s\pm$ symmetry in $\text{A}_x\text{Fe}_{2-y}\text{Se}_2$ can be caused by inter-pocket pairing, i.e. Δ changing sign between electron pockets. Another possibility¹¹ for the order parameter to change sign in $\text{A}_x\text{Fe}_{2-y}\text{Se}_2$ involves the finite energy of the coupling boson that should be higher than the binding energy of the top of the hole band at the Γ -point, but one can hardly describe the rather high T_c in the 245 family in terms of such a mechanism.

4.2. Superconducting gap

The best FeSCs for ARPES and, consequently, the systems on which the most reliable data on superconducting gap can be obtained, are LiFeAs, BKFA (and similar hole-doped compounds), and BFAP.

LiFeAs allows the most careful determination of the gap.^{62,64} Accurate measurements at 1 K have made it possible to detect the variations of Δ over the FS with a relative precision of 0.3 meV and the result is the following⁶⁴ (see Fig. 6): on the small hole-like FS at the Γ -point of $d_{xz/yz}$ origin, that, at some k_z , only touches the Fermi level, the largest superconducting energy gap of size of 6 meV opens, in agreement with tunneling spectroscopy.¹⁶¹ Along the large 2D hole-like FS of d_{xy} character the gap varies around 3.4 meV roughly as $0.5 \text{ meV} \cos(4\phi)$, with a minimum in the direction of the electron-like FS. The gap on the outer electron pocket is smaller than on the inner pocket and both vary around 3.6 meV as $0.5 \text{ meV} \cos(4\phi)$, with maxima in the direction of the Γ -point. The detected gap anisotropy is difficult to reconcile with coupling through spin fluctuations and the sign change of the order parameter, but is better fit by the model of orbital fluctuations assisted by phonons.^{154,158,159}

In BKFA, the superconducting gap has been studied by various experimental techniques,^{43,151} and the vast majority of the results can be interpreted in terms of the presence of comparable amounts of electronic states with a large gap ($\Delta_{\text{large}} = 10\text{--}11 \text{ meV}$) and with a small gap ($\Delta_{\text{small}} < 4 \text{ meV}$). The in-plane momentum dependence of the superconducting gap, determined in early ARPES studies, is the following: a large gap is located on all parts of the FS except for the outer hole-like FS sheet around the Γ -point.^{39,41} A clear correlation between the orbital character of the electronic states and their propensity to superconductivity has been observed¹⁴⁶ in hole-doped BaFe_2As_2 : the magnitude of the superconducting gap maximizes at 10.5 meV exclusively for iron $3d_{xz, yz}$ orbitals, while for others it drops to 3.5 meV (see Fig. 7). Motivated by earlier reports of a nodal gap from NMR¹⁵⁵ and angle-resolved thermal conductivity,¹⁵⁶ the superconducting gap in BFAP was measured by ARPES⁵⁷ as function of k_z , the out-of-plane momentum. A “circular line node” on the largest hole FS around the Z point at the Brillouin zone (BZ) boundary was found. This was regarded as evidence of $s\pm$ symmetry.⁵⁷ Alternatively, taking into account the observed correlation of the gap value with the orbital character of the electronic states,¹⁴⁶ the “circular line node” can be explained in terms of the positioning of an extremely small gap at the BZ boundary owing to a lack of $d_{xz/yz}$ character for the given FS sheet.

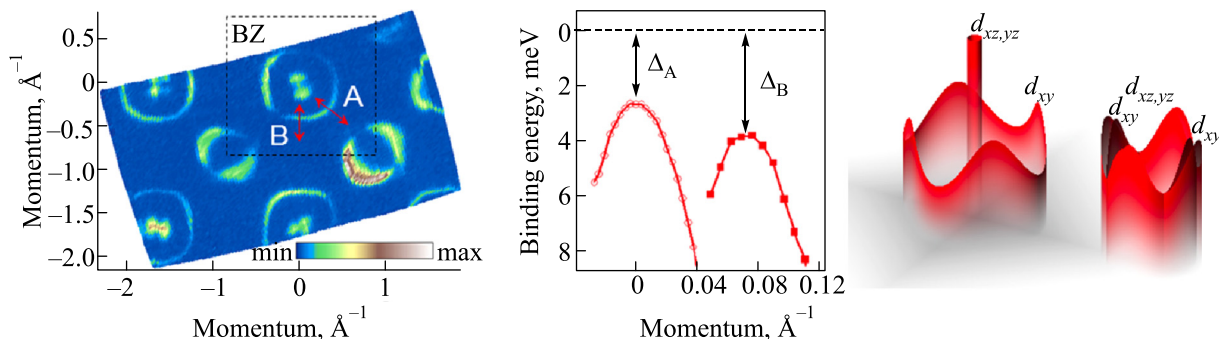


FIG. 6. Superconducting gap symmetry in LiFeAs. Experimental Fermi surface (left). The experimental dispersions (center) measured along the cuts A and B. A sketch of the distribution of the superconducting gap magnitude over the Fermi surfaces (right). After Ref. 11.

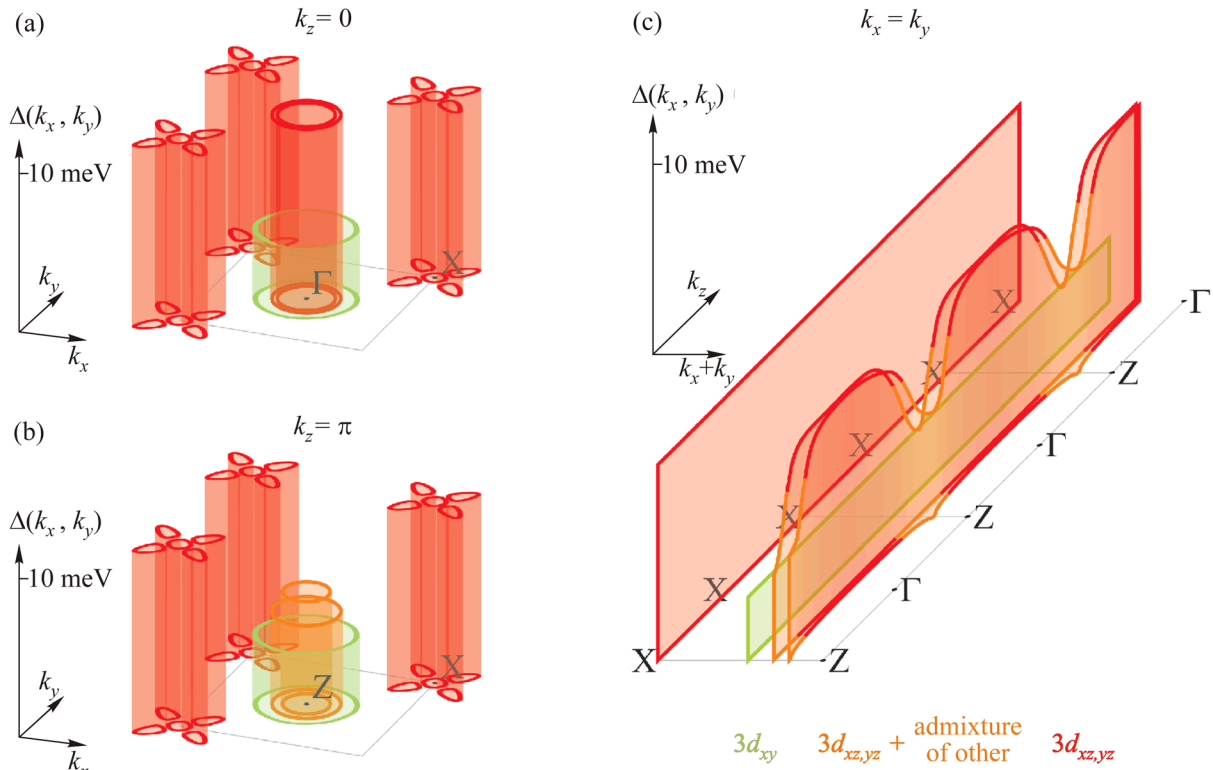


FIG. 7. Three-dimensional distribution of the superconducting gap and orbital composition of the electronic states at the Fermi level of $\text{Ba}_{1-x}\text{K}_x\text{Fe}_2\text{As}_2$ (BKFA). (a) Distribution of the superconducting gap (plotted as height) and distribution of the orbital composition for the states at the Fermi level (shown in color: $d_{xz,yz}$ —red, d_{xy} —green, $d_{xz,yz}$ with admixture of other orbitals—orange) as function of k_x and k_y at constant $k_z = 0$; (b) the same, only for $k_z = \pi$; (c) the same distributions as functions of in-plane momentum, directed along BZ diagonal, and k_z . Note the unambiguous correlation between the color and height, i.e., there is strong correlation between the orbital composition and superconducting gap magnitude. From Ref. 146.

4.3. Electronic structure and T_c

One can safely say that the major characteristic of the iron-based superconductors is their complex electronic band structure that usually results in five Fermi surface sheets (see Fig. 8): three around the center of the Fe_2As_2 BZ and two around the corners. Band structure calculations predict rather similar electronic structure for all the FeSCs.^{162,163} ARPES experiments show that this is indeed the case: one can fit the calculated bands to the experiment if they are renormalized about 3 times and shifted slightly with respect to each other.^{50,62,164,165} In this section, I focus first on the most “arpesable” LiFeAs and BKFA compounds, before discussing their electronic structure in detail.

LiFeAs. Figure 8(a) shows a fragment of the low-energy electronic band structure of LiFeAs calculated using the LMTO method in the atomic sphere approximation.¹⁶⁶ The same calculated bands but 3 times renormalized are replotted in panel (b) as dotted curves for comparison with the dispersions derived from the numerous ARPES spectra^{62,63} shown in the same panel as thick solid curves. The experimental Fermi surface is sketched in panel (c). The five bands of interest are colored in accordance to the most pronounced orbital character: Fe $3d_{xy}$, $3d_{xz}$, and $3d_{yz}$.^{167,168} These orbital characters help us identify uniquely the bands in the experimental spectra using differently polarized photons.⁶²

Comparing the results of the experiment and the renormalized calculations, one can see that the greatest difference occurs around the Γ point: the experimental d_{xy} band is shifted up about 40 meV (120 meV, in terms of the bare band

structure) while the d_{xz}/d_{yz} bands are shifted about 40 (120) meV downwards. Around the corners of the BZ (X point) the changes are different, the up-shift of the d_{xy} band at the X point is about 60 meV while the d_{xz}/d_{yz} bands are also shifted up slightly (about 10 meV). At the Fermi level, the largest hole-like FS sheet around the Γ point, formed by a d_{xy} band, is larger in the experiment than in the calculations. This is compensated by the shrunken d_{xz}/d_{yz} FSs, where the larger one has become three-dimensional, i.e. closed in the k_z direction, and the smallest one has disappeared completely. The electron-like FSs have changed only slightly, with changed character in the ΓX direction owing to a shift in the crossing of the d_{xz} and d_{xy} bands below the Fermi level; see Fig. 8(b). Thus, the experimental electronic band structure of LiFeAs has the following very important differences from the calculated one⁶²: (i) there is no FS nesting [see Fig. 4 (left)], and (ii) the vHs, the tops of the d_{xz}/d_{yz} bands at the Γ point, stays in the vicinity of the Fermi level, i.e., the system is very close to a Lifshitz transition.¹⁶⁹ The latter makes the band structure of LiFeAs similar to the structure of optimally doped $\text{Ba}(\text{Fe}_{1-x}\text{Co}_x)\text{As}_2$ (BFCA),⁴⁷ as discussed below.

BKFA. I start with the parent stoichiometric BaFe_2As_2 , for which a representative fragment of the calculated electronic band structure is shown in Fig. 8(d). It is very similar to the band structure of LiFeAs with a small complication at the bottom of the d_{xy} bands at the X point that is a consequence of body-centered tetragonal stacking of the FeAs layers instead of the simple tetragonal stacking in LiFeAs .

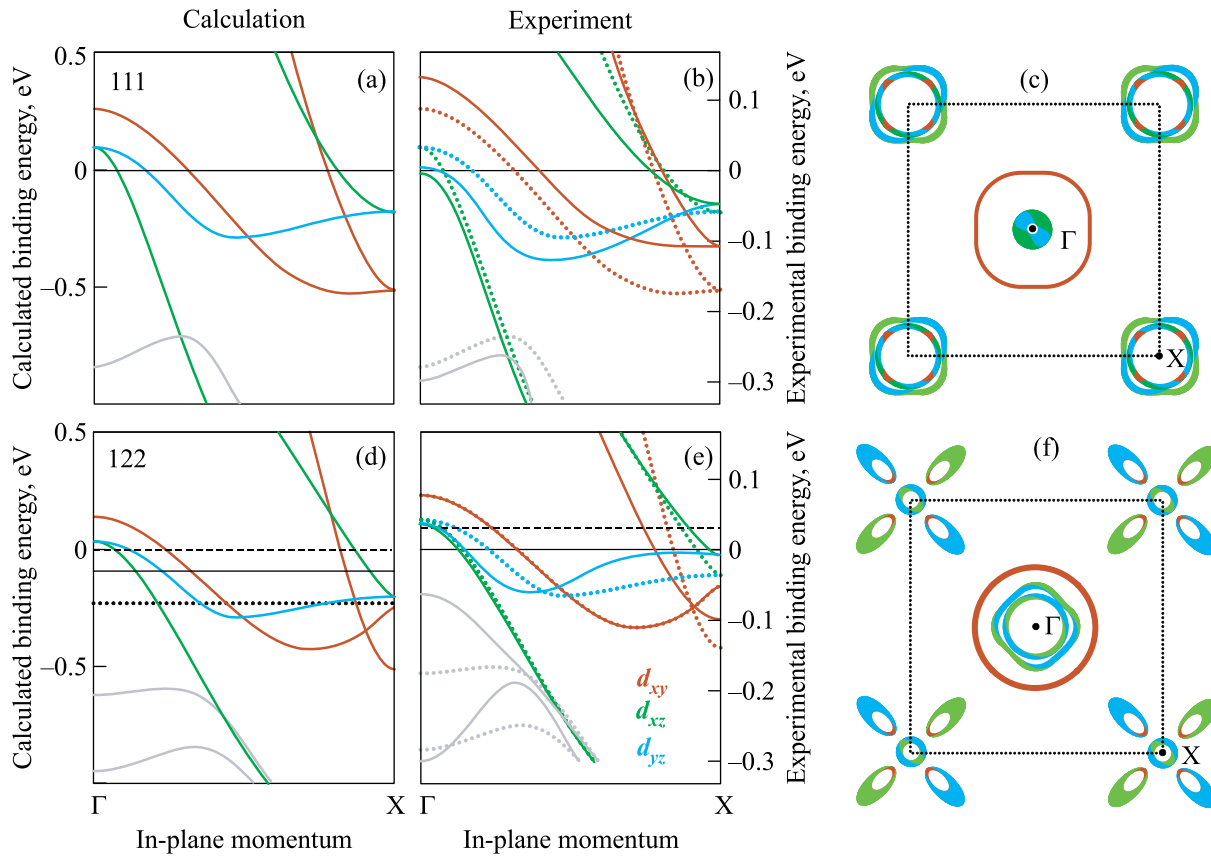


FIG. 8. Electronic band structure of LiFeAs (a)–(c), a representative 111 compound, and BaFe₂As₂ (BFA)/Ba_{0.6}K_{0.4}Fe₂As₂ (BKFA) (d)–(f), the parent/optimally doped 122 compound: the electronic bands, calculated (a), (d) and derived from ARPES data (b), (e), and the Fermi surfaces of LiFeAs (c) and BKFA (f), as seen by ARPES. The bands and FS contours are colored according to their most pronounced orbital character: Fe 3 d_{xy} , 3 d_{xz} , and 3 d_{yz} .

With the highest transition temperature ($T_c = 38$ K) and the sharpest ARPES spectra in the 122 family, the hole-doped BKFA and BNFA are the most promising and most popular objects for research on the mechanism of superconductivity in ferro-pnictides. This said, it is important to stress that the FS of the optimally doped Ba_{0.6}K_{0.4}Fe₂As₂ and Ba_{0.6}Na_{0.4}Fe₂As₂ is topologically different from the expected one: instead of two electron-like pockets around the corners of the Fe₂As₂ BZ (X and Y points) there is a propeller-like FS with the hole-like blades and a very small electron-like center,^{40,170} as shown in Fig. 4 (right). Curiously enough, despite the experimental reports of the propeller-like FS, the “parent” FS is still used in a number of theoretical models and as a basis for interpretation of experimental data on superconducting gap symmetry.

Our first interpretation of the propeller-like FS as evidence of additional electronic ordering⁴⁰ was based on temperature dependence of the photoemission intensity around the X point and on the similarity of its distribution to the parent BFA, but an interpretation based on a shift of the electronic band structure⁵⁰ has also been discussed. Now, while it seems that electronic ordering plays a certain role in spectral weight redistribution,⁴⁴ we have much more evidence for a “structural” origin of the propellers: (1) a propeller-like FS, such as shown Fig. 7(a), is routinely observed for every optimally doped BKFA or BNFA crystal we have studied. (2) In extremely overdoped KFA,^{31,54} where the magnetic ordering is not expected at all, they naturally (according to rigid band approximation) evolve to larger hole-like propellers. (3) The same propellers appear in the spectrum of the

overdoped ($T_c = 10$ K) BFCA at 90 meV below the Fermi level.¹⁷

Figure 8(e) shows the experimental bands (solid curves), derived from a number of ARPES spectra,¹⁷ on top of the bands (thin dotted curves) calculated for the parent BFA, 3 times renormalized, and shifted by 30 meV, as discussed above, to model the band structure expected for Ba_{0.6}K_{0.4}Fe₂As₂. One can see that the difference between the experimental and “expected” dispersions is even smaller than in case of LiFeAs and mainly appears near the X point as 40 meV shifts of the d_{xz}/d_{yz} bands and one of d_{xy} bands. These small shifts, however, lead to a topological Lifshitz transition of the FS and the question is how it is related to superconductivity.

Naturally, one would like to examine whether one of the peaks in the electronic density of states (DOS), related to the Lifshitz transitions, can be responsible for the enhancement of superconductivity in BKFA. Comparing the DOS calculated for the parent BFA and the model Fermi surfaces^{17,173} one can see that the chemical potential, for which the FS would be the most similar to the experimental FS of BKFA, drops in the region where the DOS of the d_{xz}/d_{yz} bands exhibits its singularities. Strictly speaking, at an energy of -228 meV the DOS is not peaked but is increasing as the energy decreases, hinting that a simple correlation between DOS and T_c , as suggested in Ref. 163, does not work for BKFA. From this procedure one can also conclude that extremely doped KFA should have a much higher DOS than any BKFA, which clearly contradicts the idea of a simple relation between the DOS and T_c . On the other hand, the high- T_c superconductivity scenario driven by interband pairing in a multiband system in

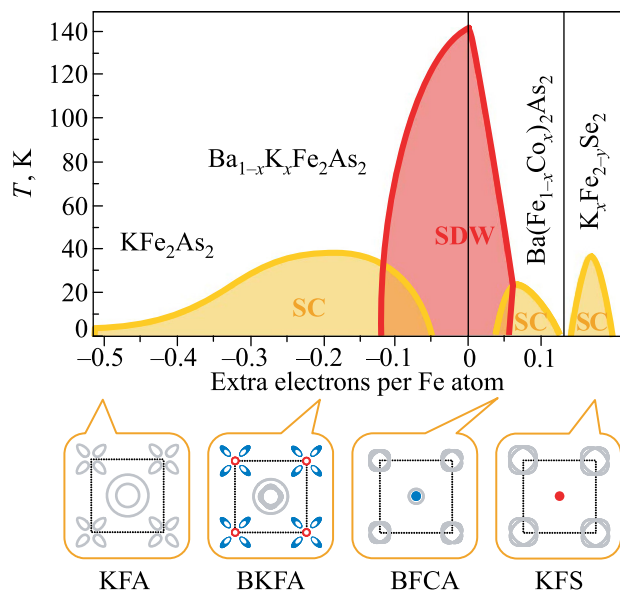


FIG. 9. Phase diagram of the 122 family of ferro-pnictides complemented by the 122(Se) family as a generalized band structure-driven diagram for the iron-based superconductors. The insets show that the Fermi surfaces for every compound close to $T_{c\max}$ are in the proximity of Lifshitz topological transitions: the corresponding FS sheets are indicated in color (blue for hole- and red for electron-like).

the proximity of a Lifshitz topological transition,^{171,172} looks like a more promising alternative for BKFA. This said, it would appear to be an extremely challenging task for chemists to proceed with further overdoping in order to reach the $d_{xz/yz}$ saddle points responsible for the largest DOS peak at -282 eV. Interestingly, the same can be suggested for LiFeAs, where the DOS¹⁷³ shows a much higher peak with the same $d_{xz/yz}$ origin.

Going back to the Lifshitz transitions in iron-based superconductors, let us review their electronic band structures that are now accessible by ARPES. Recently, a correlation of the Lifshitz transition with the onset of superconductivity has been observed in BFCA.^{46,47} The study has been mainly concentrated on the outer hole-like FS formed by d_{xy} orbitals, nevertheless, it has been also found⁴⁷ that the tops of the d_{xz}/d_{yz} bands go to the Fermi level for the samples with optimal doping and that $T_c = 24$ K. Thus, the FS of optimally doped BFCA is similar to the FS formed by d_{xz}/d_{yz} bands of LiFeAs, i.e., for the case when the Γ -centered $d_{xz/yz}$ FS pocket is in the proximity of a Lifshitz transition. One can add another 111 compound here, NaFeAs; in it the tops of d_{xz}/d_{yz} bands are also very close to the Fermi level.⁷⁰

One more example to support this picture comes from the 245 family.¹⁶³ The ARPES spectra of these compounds⁸⁹ are not very sharp yet, but one can confidently say that the bottom of the electron pocket at the center of the BZ is very close to the Fermi level; this allows us to place this family on the electron overdoped side of the generalized phase diagram, as shown in Fig. 9. Finally, we note that in all known cases the bands whose Lifshitz transitions do correlate with T_c have predominantly Fe $3d_{xz/yz}$ orbital character.

5. Conclusions

While the mechanisms of superconductivity and magnetism in FeSC are still not fully known, experimental determinations of the electronic band structure do yield some useful

conclusions. Now we can say that the electronic structure of FeSC is either clear or can be easily clarified by experiment so that one can easily fit the calculated bands to experiment data if it is permissible to renormalize them about 3 times and shift them slightly with respect to one other. Thus, we can suggest the following procedure:

$$\begin{aligned} \text{experiment} &= (\text{calculation} + \text{shifts}) \times \text{renormalization}, \\ \text{calculation} &\Rightarrow \text{orbital character}, \\ \text{shifts} &\Rightarrow \text{FS topology} + \text{nesting conditions}, \end{aligned}$$

i.e., by comparing experiments and calculations one can get the correct electronic structure with known orbital symmetry and estimate the self-energy (renormalization). From the former, one gets the Fermi surface topology needed for understanding superconductivity and the FS geometry (nesting conditions) that may or may not be important for understanding the magnetism in this case. Renormalization can provide information about the electron interactions.

Given all the electronic band structures of FeSCs that can be derived from ARPES, it has been found that the Fermi surface of every optimally doped compound (the compounds with highest T_c) has van Hove singularities of the Fe $3d_{xz/yz}$ bands in the vicinity to the Fermi level. This suggests that proximity to an electronic topological transition, known as a Lifshitz transition, for one of the multiple Fermi surfaces produces the superconductivity dome in the phase diagram. Since the parent band structure is known, one can deliberately move the essential vHs to the Fermi level by charge doping, by isovalent doping, or by pressure. Based on this empirical observation, one can predict, in particular, that hole overdoping of KFe_2As_2 and LiFeAs compounds is a possible way to increase the T_c .

To summarize, the iron-based superconductors promise interesting physics and applications. While the interplay of superconductivity and magnetism, as well as their mechanisms, are the subjects of debates and research, one thing is clear in the FeSC puzzle: the complex multi-band electronic structure of these compounds determines their rich and puzzling properties. What is important and fascinating is that this complexity seems to play a positive role in the struggle for understanding the FeSC physics and also in the search for materials with higher T_c . This is because the multiple electronic bands and the resulting complex Fermiology provide exceptionally rich ground for establishing useful empirical correlations. This is also because this electronic structure is well understood: the band structure calculations reproduce its complexity (all the bands and their symmetry) quite well. Here the role of experiment is merely to determine the exact position and renormalization for each band. This piece of experimental knowledge appears, however, to be vitally important for understanding all of the electronic properties of these new compounds.

I am pleased to dedicate this review to the 80th birthday of Professor V. V. Ereminko. I acknowledge numerous discussions with members of the ARPES group at IFW Dresden: S. V. Borisenko, D. V. Evtushinsky, and V. B. Zabolotnyy, as well as with A. Bianconi, A. V. Boris, B. Büchner, A. V. Chubukov, A. M. Gabovich, G. E. Grechnev, P. J. Hirschfeld, D. S. Inosov, T. K. Kim, Yu. V. Kopaev, M. M. Korshunov, I. I. Mazin, I. V. Morozov, I. A. Nekrasov, S. G. Ovchinnikov, E. A. Pashitskii, S. M. Ryabchenko, M. V.

Sadovskii, S. Thirupathaiah, M. A. Tanatar, and A. N. Yaresko. The project was supported by the DFG priority program SPP1458, Grants No. KN393/4, BO1912/2-1.

^{a)}Email: kordyuk@gmail.com

- ¹Y. Kamihara, T. Watanabe, M. Hirano, and H. Hosono, *J. Am. Chem. Soc.* **130**, 3296 (2008).
- ²M. V. Sadovskii, *Phys. Usp.* **51**, 1201 (2008).
- ³A. L. Ivanovskii, *Phys. Usp.* **51**, 1229 (2008).
- ⁴Y. A. Izyumov and E. Z. Kurmaev, *Phys. Usp.* **51**, 1261 (2008).
- ⁵K. Ishida, Y. Nakai, and H. Hosono, *J. Phys. Soc. Jpn.* **78**, 062001 (2009).
- ⁶I. Mazin and J. Schmalian, *Physica C* **469**, 614 (2009).
- ⁷D. C. Johnston, *Adv. Phys.* **59**, 803 (2010).
- ⁸J. Paglione and R. L. Greene, *Nat. Phys.* **6**, 645 (2010).
- ⁹H.-H. Wen and S. Li, *Ann. Rev. Condens. Matter Phys.* **2**, 121 (2011).
- ¹⁰G. R. Stewart, *Rev. Mod. Phys.* **83**, 1589 (2011).
- ¹¹P. J. Hirschfeld, M. M. Korshunov, and I. I. Mazin, *Rep. Prog. Phys.* **74**, 124508 (2011).
- ¹²A. Chubukov, *Ann. Rev. Condens. Matter Phys.* **3**, 57 (2012).
- ¹³M. Putti, I. Pallecchi, E. Bellingeri, M. R. Cimberle, M. Tropeano, C. Ferdeghini, A. Palenzona, C. Tarantini, A. Yamamoto, J. Jiang, J. Jaroszynski, F. Kametani, D. Abrahimov, A. Polyanskii, J. D. Weiss, E. E. Hellstrom, A. Gurevich, D. C. Larbalestier, R. Jin, B. C. Sales, A. S. Sefat, M. A. McGuire, D. Mandrus, P. Cheng, Y. Jia, H. H. Wen, S. Lee and C. B. Eom, *Supercond. Sci. Technol.* **23**, 034003 (2010).
- ¹⁴P. J. W. Moll, R. Puzniak, F. Balakirev, K. Rogacki, J. Karpinski, N. D. Zhigadlo, and B. Batlogg, *Nat. Mater.* **9**, 628 (2010).
- ¹⁵A. Gurevich, *Rep. Prog. Phys.* **74**, 124501 (2011).
- ¹⁶U. Patel, J. Hua, S. H. Yu, S. Avci, Z. L. Xiao, H. Claus, J. Schlueter, V. V. Vlasko-Vlasov, U. Welp, and W. K. Kwok, *Appl. Phys. Lett.* **94**, 082508 (2009).
- ¹⁷A. A. Kordyuk, A. A. Kordyuk, V. B. Zabolotnyy, D. V. Evtushinsky, A. N. Yaresko, B. Büchner, S. V. Borisenko, e-print arXiv:1111.0288 (2011).
- ¹⁸A. A. Kordyuk and S. V. Borisenko, *Fiz. Nizk. Temp.* **32**, 401 (2006) [*Low Temp. Phys.* **32**, 298 (2006)].
- ¹⁹S. Nandi, S. Nandi, M. G. Kim, A. Kreyssig, R. M. Fernandes, D. K. Pratt, A. Thaler, N. Ni, S. L. Bud'ko, P. C. Canfield, J. Schmalian, R. J. McQueeney, and A. I. Goldman, *Phys. Rev. Lett.* **104**, 057006 (2010).
- ²⁰H. Luetkens, H.-H. Klauss, M. Kraken, F. J. Litterst, T. Dellmann, R. Klingeler, C. Hess, R. Khasanov, A. Amato, C. Baines, M. Kosmala, O. J. Schumann, M. Braden, J. Hamann-Borrero, N. Leps, A. Kondrat, G. Behr, J. Werner, and B. Büchner, *Nature Mater.* **8**, 305 (2009).
- ²¹N. Katayama, N. Katayama, S. Ji, D. Louca, S. Lee, M. Fujita, T. J. Sato, J. Wen, Zh. Xu, G. Gu, G. Xu, Z. Lin, M. Enoki, S. Chang, K. Yamada, and J. M. Tranquada, *J. Phys. Soc. Jpn.* **79**, 113702 (2010).
- ²²S. Jiang, H. Xing, G. Xuan, C. Wang, Zh. Ren, Ch. Feng, J. Dai, Zh. Xu and G. Cao, *J. Phys.: Condens. Matter* **21**, 382203 (2009).
- ²³H. Eschrig, A. Lankau, and K. Koepnik, *Phys. Rev. B* **81**, 155447 (2010).
- ²⁴C. Liu, Y. Lee, A. D. Palczewski, J.-Q. Yan, T. Kondo, B. N. Harmon, R. W. McCallum, T. A. Lograsso, and A. Kaminski, *Phys. Rev. B* **82**, 075135 (2010).
- ²⁵M. Rotter, M. Tegel, and D. Johrendt, *Phys. Rev. Lett.* **101**, 107006 (2008).
- ²⁶A. S. Sefat, R. Jin, M. A. McGuire, B. C. Sales, D. J. Singh, and D. Mandrus, *Phys. Rev. Lett.* **101**, 117004 (2008).
- ²⁷N. Ni, M. E. Tillman, J.-Q. Yan, A. Kracher, S. T. Hannahs, S. L. Bud'ko, and P. C. Canfield, *Phys. Rev. B* **78**, 214515 (2008).
- ²⁸V. Brouet, V. Brouet, M. Marsi, B. Mansart, A. Nicolaou, A. Taleb-Ibrahimi, P. Le Fèvre, F. Bertran, F. Rullier-Albenque, A. Forget, and D. Colson, *Phys. Rev. B* **80**, 165115 (2009).
- ²⁹T. Kondo, R. M. Fernandes, R. Khasanov, Ch. Liu, A. D. Palczewski, N. Ni, M. Shi, A. Bostwick, E. Rotenberg, J. Schmalian, S. L. Bud'ko, P. C. Canfield, and A. Kaminski, *Phys. Rev. B* **81**, 060507 (2010).
- ³⁰M. Rotter, M. Tegel, D. Johrendt, I. Schellenberg, W. Hermes, and R. Pöttgen, *Phys. Rev. B* **78**, 020503 (2008).
- ³¹T. Sato, K. Nakayama, Y. Sekiba, P. Richard, Y.-M. Xu, S. Souma, T. Takahashi, G. F. Chen, J. L. Luo, N. L. Wang, and H. Ding, *Phys. Rev. Lett.* **103**, 047002 (2009).
- ³²R. Cortes-Gil, D. R. Parker, M. J. Pitcher, J. Hadermann, and S. J. Clarke, *Chem. Mater.* **22**, 4304 (2010).
- ³³S. Aswartham, M. Abdel-Hafiez, D. Bombor, M. Kumar, A. U. B. Wolter, C. Hess, D. V. Evtushinsky, V. B. Zabolotnyy, A. A. Kordyuk, T. K. Kim, S. V. Borisenko, G. Behr, B. Büchner, and S. Wurmehl, e-print arXiv:1203.0143 (2012).
- ³⁴G. Wu, M. Abdel-Hafiez, D. Bombor, M. Kumar, A. U. B. Wolter, C. Hess, D. V. Evtushinsky, V. B. Zabolotnyy, A. A. Kordyuk, T. K. Kim, S. V. Borisenko, G. Behr, B. Büchner, and S. Wurmehl, *J. Phys.: Condens. Matter* **20**, 422201 (2008).
- ³⁵T. Park, E. Park, H. Lee, T. Klimczuk, E. D. Bauer, F. Ronning, and J. D. Thompson, *J. Phys.: Condens. Matter* **20**, 322204 (2008).
- ³⁶Z. Ren, Q. Tao, Sh. Jiang, Ch. Feng, C. Wang, J. Dai, G. Cao, and Z. Xu, *Phys. Rev. Lett.* **102**, 137002 (2009).
- ³⁷P. Richard, T. Sato, K. Nakayama, T. Takahashi, and H. Ding, *Rep. Prog. Phys.* **74**, 124512 (2011).
- ³⁸C. Liu, G. D. Samolyuk, Y. Lee, N. Ni, Takeshi Kondo, A. F. Santander-Syro, S. L. Bud'ko, J. L. McChesney, E. Rotenberg, T. Valla, A. V. Fedorov, P. C. Canfield, B. N. Harmon, and A. Kaminski, *Phys. Rev. Lett.* **101**, 177005 (2008).
- ³⁹H. Ding, P. Richard, K. Nakayama, K. Sugawara, T. Arakane, Y. Sekiba, A. Takayama, S. Souma, T. Sato, T. Takahashi, Z. Wang, X. Dai, Z. Fang, G. F. Chen, J. L. Luo and N. L. Wang, *Europhys. Lett.* **83**, 47001 (2008).
- ⁴⁰V. B. Zabolotnyy, D. S. Inosov, D. V. Evtushinsky, A. Koitzsch, A. A. Kordyuk, G. L. Sun, J. T. Park, D. Haug, V. Hinkov, A. V. Boris, C. T. Lin, M. Knupfer, A. N. Yaresko, B. Büchner, A. Varykhalov, R. Follath, and S. V. Borisenko, *Nature* **457**, 569 (2009).
- ⁴¹D. V. Evtushinsky, D. S. Inosov, V. B. Zabolotnyy, A. Koitzsch, M. Knupfer, B. Büchner, M. S. Viazovska, G. L. Sun, V. Hinkov, A. V. Boris, C. T. Lin, B. Keimer, A. Varykhalov, A. A. Kordyuk, and S. V. Borisenko, *Phys. Rev. B* **79**, 054517 (2009).
- ⁴²P. Richard, T. Sato, K. Nakayama, S. Souma, T. Takahashi, Y.-M. Xu, G. F. Chen, J. L. Luo, N. L. Wang, and H. Ding, *Phys. Rev. Lett.* **102**, 047003 (2009).
- ⁴³D. V. Evtushinsky, D. S. Inosov, V. B. Zabolotnyy, M. S. Viazovska, R. Khasanov, A. Amato, H.-H. Klauss, H. Luetkens, Ch. Niedermayer, G. L. Sun, V. Hinkov, C. T. Lin, A. Varykhalov, A. Koitzsch, M. Knupfer, B. Büchner, A. A. Kordyuk and S. V. Borisenko, *New J. Phys.* **11**, 055069 (2009).
- ⁴⁴D. V. Evtushinsky, A. A. Kordyuk, V. B. Zabolotnyy, D. S. Inosov, T. K. Kim, B. Büchner, H. Luo, Zh. Wang, H.-H. Wen, G. Sun, Ch. Lin, and S. V. Borisenko, *J. Phys. Soc. Jpn.* **80**, 023710 (2011).
- ⁴⁵S. Thirupathaiah, S. de Jong, R. Ovsyannikov, H. A. Dürr, A. Varykhalov, R. Follath, Y. Huang, R. Huisman, M. S. Golden, Yu-Zhong Zhang, H. O. Jeschke, R. Valentí, A. Erb, A. Gloskovskii, and J. Fink, *Phys. Rev. B* **81**, 104512 (2010).
- ⁴⁶C. Liu, T. Kondo, R. M. Fernandes, A. D. Palczewski, E. D. Mun, N. Ni, A. N. Thaler, A. Bostwick, E. Rotenberg, J. Schmalian, S. L. Bud'ko, P. C. Canfield, and A. Kaminski, *Nature Phys.* **6**, 419 (2010).
- ⁴⁷C. Liu, T. Kondo, R. M. Fernandes, A. D. Palczewski, E. D. Mun, N. Ni, A. N. Thaler, A. Bostwick, E. Rotenberg, J. Schmalian, S. L. Bud'ko, P. C. Canfield, and A. Kaminski, *Phys. Rev. B* **84**, 020509 (2011).
- ⁴⁸M. Yi, D. Lu, J.-H. Chu, J. G. Analytis, A. P. Sorini, A. F. Kemper, B. Moritz, S.-K. Mo, R. G. Moore, M. Hashimoto, W.-Sh. Lee, Z. Hussain, Th. P. Devereaux, I. R. Fisher, and Zh.-X. Shen, *Proc. Natl. Acad. Sci.* **108**, 6878 (2011).
- ⁴⁹E. van Heumen, J. Vuorinen, K. Koepnik, F. Massee, Y. Huang, M. Shi, J. Klei, J. Goedkoop, M. Lindroos, J. van den Brink, and M. S. Golden, *Phys. Rev. Lett.* **106**, 027002 (2011).
- ⁵⁰M. Yi, D. H. Lu, J. G. Analytis, J.-H. Chu, S.-K. Mo, R.-H. He, R. G. Moore, X. J. Zhou, G. F. Chen, J. L. Luo, N. L. Wang, Z. Hussain, D. J. Singh, I. R. Fisher, and Z.-X. Shen, *Phys. Rev. B* **80**, 024515 (2009).
- ⁵¹J. Fink, S. Thirupathaiah, R. Ovsyannikov, H. A. Dürr, R. Follath, Y. Huang, S. de Jong, M. S. Golden, Yu-Zh. Zhang, H. O. Jeschke, R. Valentí, C. Felser, S. D. Farahani, M. Rotter, and D. Johrendt, *Phys. Rev. B* **79**, 155118 (2009).
- ⁵²P. Richard, K. Nakayama, T. Sato, M. Neupane, Y.-M. Xu, J. H. Bowen, G. F. Chen, J. L. Luo, N. L. Wang, X. Dai, Z. Fang, H. Ding, and T. Takahashi, *Phys. Rev. Lett.* **104**, 137001 (2010).
- ⁵³Y. Kim, H. Oh, Ch. Kim, D. Song, W. Jung, B. Kim, H. J. Choi, Ch. Kim, B. Lee, S. Khim, H. Kim, K. Kim, J. Hong, and Y. Kwon, *Phys. Rev. B* **83**, 064509 (2011).
- ⁵⁴T. Yoshida, I. Nishi, A. Fujimori, M. Yi, R. G. Moore, D.-H. Lu, Z.-X. Shen, K. Kihou, P. M. Shirage, H. Kito, C. H. Lee, A. Iyo, H. Eisaki, H. Harima, *J. Phys. Chem. Solids* **72**, 465 (2011).
- ⁵⁵C. Liu, Takeshi Kondo, N. Ni, A. D. Palczewski, A. Bostwick, G. D. Samolyuk, R. Khasanov, M. Shi, E. Rotenberg, S. L. Bud'ko, P. C. Canfield, and A. Kaminski, *Phys. Rev. Lett.* **102**, 167004 (2009).
- ⁵⁶T. Yoshida, I. Nishi, S. Ideta, A. Fujimori, M. Kubota, K. Ono, S. Kasahara, T. Shibauchi, T. Terashima, Y. Matsuda, H. Ikeda, and R. Arita, *Phys. Rev. Lett.* **106**, 117001 (2011).

- ¹²⁰S. Iikubo, M. Fujita, S. Niitaka, and H. Takagi, *J. Phys. Soc. Jpn.* **78**, 103704 (2009).
- ¹²¹C. Lester, Jiun-Haw Chu, J. G. Analytis, T. G. Perring, I. R. Fisher, and S. M. Hayden, *Phys. Rev. B* **81**, 064505 (2010).
- ¹²²H.-F. Li, D. Vaknin, R. M. Fernandes, D. L. Abernathy, M. B. Stone, D. K. Pratt, W. Tian, Y. Qiu, N. Ni, S. O. Diallo, J. L. Zarestky, S. L. Bud'ko, P. C. Canfield, and R. J. McQueeney, *Phys. Rev. B* **82**, 140503 (2010).
- ¹²³D. N. Argyriou, A. Hiess, A. Akbari, I. Eremin, M. M. Korshunov, J. Hu, B. Qian, Z. Mao, Y. Qiu, C. Broholm, and W. Bao, *Phys. Rev. B* **81**, 220503 (2010).
- ¹²⁴S. O. Diallo, D. K. Pratt, R. M. Fernandes, W. Tian, J. L. Zarestky, M. Lumsden, T. G. Perring, C. L. Broholm, N. Ni, S. L. Bud'ko, P. C. Canfield, H.-F. Li, D. Vaknin, A. Kreyssig, A. I. Goldman, and R. J. McQueeney, *Phys. Rev. B* **81**, 214407 (2010).
- ¹²⁵B. Vignolle, S. M. Hayden, D. F. McMorro, H. M. Rønnow, B. Lake, C. D. Frost, and T. G. Perring, *Nat. Phys.* **3**, 163 (2007).
- ¹²⁶P. Monthoux and D. J. Scalapino, *Phys. Rev. Lett.* **72**, 1874 (1994).
- ¹²⁷M. M. Korshunov and I. Eremin, *Phys. Rev. B* **78**, 140509 (2008).
- ¹²⁸T. A. Maier and D. J. Scalapino, *Phys. Rev. B* **78**, 020514 (2008).
- ¹²⁹A. D. Christianson, E. A. Goremychkin, R. Osborn, S. Rosenkranz, M. D. Lumsden, C. D. Malliakas, I. S. Todorov, H. Claus, D. Y. Chung, M. G. Kanatzidis, R. I. Bewley, and T. Guidi, *Nature* **456**, 930 (2008).
- ¹³⁰M. D. Lumsden, A. D. Christianson, D. Parshall, M. B. Stone, S. E. Nagler, G. J. MacDougall, H. A. Mook, K. Lokshin, T. Egami, D. L. Abernathy, E. A. Goremychkin, R. Osborn, M. A. McGuire, A. S. Sefat, R. Jin, B. C. Sales, and D. Mandrus, *Phys. Rev. Lett.* **102**, 107005 (2009).
- ¹³¹D. S. Inosov, J. T. Park, P. Bourges, D. L. Sun, Y. Sidis, A. Schneidewind, K. Hradil, D. Haug, C. T. Lin, B. Keimer, and V. Hinkov, *Nat. Phys.* **6**, 178 (2010).
- ¹³²S.-H. Lee, Guangyong Xu, W. Ku, J. S. Wen, C. C. Lee, N. Katayama, Z. J. Xu, S. Ji, Z. W. Lin, G. D. Gu, H.-B. Yang, P. D. Johnson, Z.-H. Pan, T. Valla, M. Fujita, T. J. Sato, S. Chang, K. Yamada, and J. M. Tranquada, *Phys. Rev. B* **81**, 220502 (2010).
- ¹³³J. T. Park, G. Friemel, Yuan Li, J.-H. Kim, V. Tsurkan, J. Deisenhofer, H.-A. Krug von Nidda, A. Loidl, A. Ivanov, B. Keimer, and D. S. Inosov, *Phys. Rev. Lett.* **107**, 177005 (2011).
- ¹³⁴D. S. Inosov, S. V. Borisenko, I. Eremin, A. A. Kordyuk, V. B. Zabolotnyy, J. Geck, A. Koitzsch, J. Fink, M. Knupfer, B. Büchner, H. Berger, and R. Follath, *Phys. Rev. B* **75**, 172505 (2007).
- ¹³⁵S. Onari, H. Kontani, and M. Sato, *Phys. Rev. B* **81**, 060504 (2010).
- ¹³⁶T. Timusk and B. Statt, *Rep. Prog. Phys.* **62**, 61 (1999).
- ¹³⁷S. V. Borisenko, A. A. Kordyuk, A. N. Yaresko, V. B. Zabolotnyy, D. S. Inosov, R. Schuster, B. Büchner, R. Weber, R. Follath, L. Patthey, and H. Berger, *Phys. Rev. Lett.* **100**, 196402 (2008).
- ¹³⁸A. A. Kordyuk, S. V. Borisenko, V. B. Zabolotnyy, R. Schuster, D. S. Inosov, D. V. Evtushinsky, A. I. Plyushchay, R. Follath, A. Varykhalov, L. Patthey, and H. Berger, *Phys. Rev. B* **79**, 020504 (2009).
- ¹³⁹S. Hufner, M. A. Hossain, A. Damascelli, and G. A. Sawatzky, *Rep. Prog. Phys.* **71**, 062501 (2008).
- ¹⁴⁰M. A. Tanatar, N. Ni, A. Thaler, S. L. Bud'ko, P. C. Canfield, and R. Prozorov, *Phys. Rev. B* **82**, 134528 (2010).
- ¹⁴¹A. L. Solov'ev, S. L. Sidorov, V. Yu. Tarenkov, and A. I. D'yachenko, *Fiz. Nizk. Temp.* **35**, 1055 (2009) [*Low Temp. Phys.* **35**, 826 (2009)].
- ¹⁴²T. Sato, S. Souma, K. Nakayama, K. Terashima, K. Sugawara, T. Takahashi, Y. Kamihara, M. Hirano, and H. Hosono, *J. Phys. Soc. Jpn.* **77**, 063708 (2008).
- ¹⁴³H.-Y. Liu, X.-W. Jia, W.-T. Zhang, L. Zhao, J.-Q. Meng, G.-D. Liu, X.-L. Dong, G. Wu, R.-H. Liu, X.-H. Chen, Z.-A. Ren, W. Yi, G.-C. Che, G.-F. Chen, N.-L. Wang, G.-L. Wang, Y. Zhou, Y. Zhu, X.-Y. Wang, Z.-X. Zhao, Z.-Y. Xu, C.-T. Chen, and X.-J. Zhou, *Chin. Phys. Lett.* **25**, 3761 (2008).
- ¹⁴⁴Y.-M. Xu, P. Richard, K. Nakayama, T. Kawahara, Y. Sekiba, T. Qian, M. Neupane, S. Souma, T. Sato, T. Takahashi, H.-Q. Luo, H.-H. Wen, G.-F. Chen, N.-L. Wang, Z. Wang, Z. Fang, X. Dai, H. Ding, *Nat. Commun.* **2**, 392 (2011).
- ¹⁴⁵T. Shimojima, F. Sakaguchi, K. Ishizaka, Y. Ishida, T. Kiss, M. Okawa, T. Togashi, C.-T. Chen, S. Watanabe, M. Arita, K. Shimada, H. Namatame, M. Taniguchi, K. Ohgushi, S. Kasahara, T. Terashima, T. Shibauchi, Y. Matsuda, A. Chainani, and S. Shin, *Science* **332**, 564 (2011).
- ¹⁴⁶D. V. Evtushinsky, V. B. Zabolotnyy, T. K. Kim, A. A. Kordyuk, A. N. Yaresko, J. Maletz, S. Aswartham, S. Wurmehl, A. V. Boris, D. L. Sun, C. T. Lin, B. Shen, H. H. Wen, A. Varykhalov, R. Follath, B. Büchner, and S. V. Borisenko, e-print arXiv:1204.2432v1 (2012).
- ¹⁴⁷Y. Yin, M. Zech, T. L. Williams, and J. E. Hoffman, *Physica C* **469**, 535 (2009).
- ¹⁴⁸F. Massee, Y. K. Huang, J. Kaas, E. van Heumen, S. de Jong, R. Huisman, H. Luigjes, J. B. Goedkoop, and M. S. Golden, *Europhys. Lett.* **92**, 57012 (2010).
- ¹⁴⁹A. S. Sefat, *Rep. Prog. Phys.* **74**, 124502 (2011).
- ¹⁵⁰F. Hardy, P. Burger, T. Wolf, R. A. Fisher, P. Schweiss, P. Adelman, R. Heid, R. Fromknecht, R. Eder, D. Ernst, H. v. Löhneysen, and C. Meingast, *Europhys. Lett.* **91**, 47008 (2010).
- ¹⁵¹P. Popovich, A. V. Boris, O. V. Dolgov, A. A. Golubov, D. L. Sun, C. T. Lin, R. K. Kremer, and B. Keimer, *Phys. Rev. Lett.* **105**, 027003 (2010).
- ¹⁵²H. Okabe, N. Takeshita, K. Horigane, T. Muranaka, and J. Akimitsu, *Phys. Rev. B* **81**, 205119 (2010).
- ¹⁵³I. I. Mazin, D. J. Singh, M. D. Johannes, and M. H. Du, *Phys. Rev. Lett.* **101**, 057003 (2008).
- ¹⁵⁴S. Onari and H. Kontani, *Phys. Rev. Lett.* **103**, 177001 (2009).
- ¹⁵⁵Y. Nakai, T. Iye, Sh. Kitagawa, K. Ishida, Sh. Kasahara, T. Shibauchi, Yu. Matsuda, and T. Terashima, *Phys. Rev. B* **81**, 020503 (2010).
- ¹⁵⁶M. Yamashita, Y. Senshu, T. Shibauchi, S. Kasahara, K. Hashimoto, D. Watanabe, H. Ikeda, T. Terashima, I. Vekhter, A. B. Vorontsov, and Y. Matsuda, *Phys. Rev. B* **84**, 060507 (2011).
- ¹⁵⁷A. B. Vorontsov, M. G. Vavilov, and A. V. Chubukov, *Phys. Rev. B* **81**, 174538 (2010).
- ¹⁵⁸H. Kontani and S. Onari, *Phys. Rev. Lett.* **104**, 157001 (2010).
- ¹⁵⁹Y. Yanagi, Y. Yamakawa, and Y. Ōno, *Phys. Rev. B* **81**, 054518 (2010).
- ¹⁶⁰M. Khodas and A. V. Chubukov, *Phys. Rev. Lett.* e-print arXiv:1202.5563 (2012).
- ¹⁶¹T. Hanke, S. Sykora, R. Schlegel, D. Baumann, L. Harnagea, S. Wurmehl, M. Daghofer, B. Büchner, J. van den Brink, and Ch. Hess, *Phys. Rev. Lett.* **108**, 127001 (2012).
- ¹⁶²O. K. Andersen and L. Boeri, *Ann. Phys.* **523**, 8 (2011).
- ¹⁶³M. V. Sadovskii, E. Z. Kuchinskii, and I. A. Nekrasov, e-print arXiv:1106.3707v1 (2011).
- ¹⁶⁴H. Ding, K. Nakayama, P. Richard, S. Souma, T. Sato, T. Takahashi, M. Neupane, Y.-M. Xu, Z.-H. Pan, A. V. Fedorov, Z. Wang, X. Dai, Z. Fang, G. F. Chen, J. L. Luo, and N. L. Wang, *J. Phys.: Condens. Matter* **23**, 135701 (2011).
- ¹⁶⁵S. V. Borisenko, A. A. Kordyuk, V. B. Zabolotnyy, D. V. Evtushinsky, T. K. Kim, B. Büchner, A. N. Yaresko, V. D. Borisenko, and H. Berger, *J. Phys. Chem. Solids* **72**, 562 (2011).
- ¹⁶⁶O. K. Andersen, *Phys. Rev. B* **12**, 3060 (1975).
- ¹⁶⁷P. A. Lee and X.-G. Wen, *Phys. Rev. B* **78**, 144517 (2008).
- ¹⁶⁸S. Graser, T. A. Maier, P. J. Hirschfeld, and D. J. Scalapino, *New J. Phys.* **11**, 025016 (2009).
- ¹⁶⁹I. M. Lifshitz, *Zh. Eksp. Teor. Fiz.* **38**, 1569 (1960) [*Sov. Phys. JETP* **11**, 1130 (1960)].
- ¹⁷⁰V. B. Zabolotnyy, D. V. Evtushinsky, A. A. Kordyuk, D. S. Inosov, A. Koitzsch, A. V. Boris, G. L. Sun, C. T. Lin, M. Knupfer, B. Büchner, A. Varykhalov, R. Follath, and S. V. Borisenko, *Physica C: Supercond.* **469**, 448 (2009).
- ¹⁷¹D. Innocenti, N. Poccia, A. Ricci, A. Valletta, S. Caprara, A. Perali, and A. Bianconi, *Phys. Rev. B* **82**, 184528 (2010).
- ¹⁷²D. Innocenti, S. Caprara, N. Poccia, A. Ricci, A. Valletta, and A. Bianconi, *Supercond. Sci. Technol.* **24**, 015012 (2011).
- ¹⁷³For more details, see www.imp.kiev.ua/~kord/papers/FPS11.

This article was published in English in the original Russian journal. Reproduced here with stylistic changes by AIP.